Title

3-inlet Flow-Focusing Droplet Generator Enables Longtime Production of Microporous Annealed Particle Gel with A Range of Stiffness and Size

Author

Yang, Wei

Publication Date

2017

Peer reviewed|Thesis/dissertation

UNIVERSITY OF CALIFORNIA

Los Angeles

3-inlet Flow-Focusing Droplet Generator Enables Longtime Production of Microporous Annealed Particle Gel with A Range of Stiffness and Size

A thesis submitted in partial satisfaction

of the requirements for the degree Master of Science in

Bioengineering

by

Wei Yang

2017

ABSTRACT OF THE THESIS

3-inlet Flow-Focusing Droplet Generator Enables Longtime Production of Microporous Annealed Particle Gel with A Range of Stiffness and Size

by

Wei Yang

Master of Science in Bioengineering

University of California, Los Angeles, 2017

Professor Dino Di Carlo, Chair

Injectable hydrogels are widely used as in situ scaffolds to support tissue regrowth but suffers from degradation before tissue reformation. As shown in our last paper, microporous Annealed Particle (MAP) gels can provide a stably linked interconnected network for tissue regrowth. While current applications of MAP gel composed of 4-arm poly(ethylene) glycol-vinyl sulphone (PEG-VS) backbone is limited to mimicking soft tissues new backbone material 8-arm PEG-VS increases the range of gel stiffness. Stiffer gel scaffold facilitates cell infiltration rate and expands application to tissues with greater mechanical movement. However, backbone and cross-linker materials can react in the channel and form polymers due to transverse diffusion, which causes jetting in the device and interrupts monodisperse droplet production. Here we present a three-inlet flow-focusing droplet generator which can prevent polymerization in the channel by controlling the width of a middle buffer stream. We have shown that it enables 4 times longer production time for

previous material and at least 2 times longer production time for new material. MAP gel with a higher stiffness and annealing force is achieved using the 3-inlet device. The 3-inlet device empowers mass production of MAP gel, leading to higher reproducibility of MAP gel related research studies. The study of the middle buffer stream gives ideas to other flow-focusing microfluidics system where two reactants need to be separated before encapsulation in droplets.

The thesis of Wei Yang is approved.

Chang-Jin Kim

Song Li

Dino Di Carlo, Committee Chair

University of California, Los Angeles

2017

Dedication

Mom, Dad, and Kylie

Table of Contents

Acknowledgements

Thanks to Dr. Westbrook Weaver for developing the technology of Microporous Annealed Particle gel so that I can work on the amazing technology.

I am grateful for Jaekyung Koh for teaching me the technology of fabricating MAP gel Particles and measuring its mechanical properties, and providing support and advice to my project.

I am especially thankful to Professor Dino Di Carlo for his mentorship, support and exceptional kindness.

Thanks to the precious friends in Di Carlo lab for their encouragement, suggestions, support and inspiration:

Manjima Dhar, Dr. Harsha Kittur, Dr Janay Kong, Armin Karimi, Joe de Rutte, Dr. Kahlen Ouyang, Dr. Carson Riche, Dr. Soroush Kahkeshani, Edward Pao, Dr. Hamed Haddadi, Johnathan Lin, Dr. Kah Ping Tay, Dr. Chueh-Yu Wu, Dr. Donghyuk Kim, Coleman Murray, Dr. Oladunni Adeyiga, Dr. Ivan Pushkarsky, Dr. Ming Li, Hector E Munoz, Reem Khojah.

Lastly, I am extremely grateful to my friends and my family for their constant love and support.

I. Introduction

In tissue engineering, it is important to match degradation rate of scaffold and cell infiltration rate because sufficient scaffolding should remain to support tissue ingrowth while degrade in time to allow cell infiltration and prevent fibrosis.[1,2] For conventional gel scaffold, cell invasion and tissue regeneration are limited by the rate of cell-mediated degradation due to the small mesh size. [3] Microporous Annealed Particle(MAP) gel circumvents the need for degradation by synthesizing the gel scaffold using a bottom-up approach. MAP gel is composed of monodisperse microparticle building blocks, which form a stably linked microporous gel network of micropores where cells from surrounding tissues can migrate. Therefore, MAP gel provides a robust way to achieve cell infiltration and bulk tissue integration. [4]

Monodisperse MAP gel droplets are fabricated by microfluidics water-in-oil emulsion. Individual MAP gel particles are synthesized by reactions of multi-arm poly(ethylene)glycol–vinyl sulphone (PEG–VS) and dithiol cross-linkers through a Michael type reaction. As depicted in Fig.1A, PEG-VS and cross-linker are injected into two inlet channels and then reach co-flow before they are segmented into droplets at the intersection. Droplets anneal with each other either through an enzymatic reaction described in a previous paper [4] or a light based radical polymerization [5]. Since microfluidics droplet generation enables tight control of microscale chemical reactions, we are able to tailor chemical and physical properties of individual microparticles which can then form gel scaffold with precisely tuned properties. The degradability of the gel scaffold can also be controlled by using a degradable matrix metalloprotease-sensitive peptide sequences (MMP) cross-linker or a non-degradable PEG-dithiol cross-linker.

MAP gel used in a previous paper (5wt% 4-arm) has a storage modulus of 350Pa after annealing. [4] Its application is limited to mimicking Extracellular Matrix (ECM) of soft tissue, such as skin. The elastic modulus of rat myocardium is 590 ± 22 kPa [6]. Scaffold with modulus one order below that of myocardium would facilitate mechanical stimulation of engrafted cells in vivo[7] Moreover, fibrotic lungs, fibrotic intestines, and fibrotic livers have been evaluated to have elastic modulus value ranged

from approximately 1–3 kPa for normal tissue to approximately 17–22 kPa for fibrotic tissue.[8] On the other hand, stiffer gel increases cell spreading [9] , making it a desired material to support growth of anchorage-dependent cells. [10] Moreover, it has been shown that cells commit to specific lineage in response to the stiffness of their environment. Therefore, A wider stiffness range is highly desired for tissue regeneration in tissues of different stiffness, cancer cell culture [8,10], study of pathogenesis involving cell migration in between tissues [8] and directed stem cell differentiation to different lineages. [11,12]

We have two approaches to achieve a wide range of stiffness for MAP gel particles. The first one is to tune the mass concentration (wt%, mass/volume) of PEG-VS molecule and the corresponding mass concentration of cross-linker, so that more crosslinks are introduced to the polymer network of MAP gel microparticles. For the second approach, we introduce a new backbone material 8-arm PEG-VS. For a given mass concentration of PEG molecule, 8-arm PEG-VS has twice as many reactive vinyl sulfone groups than 4-arm PEG-VS does. Therefore, we are able to achieve twice as many crosslinking sites as before for a given mass concentration and push the upper limit of stiffness range even further. (Fig.1C)

The 2-inlet flow-focusing droplet generator is able to produce monodisperse MAP gel droplets with defined size and stiffness. However, its ability to achieve mass production of MAP gel microparticles for a long time is limited by fast polymerization of reactants in the channel. (Fig.2A) PEG-VS solution and cross-linker solution co-flow before being encapsulated into droplets. Transverse diffusion of the two reactant molecules at the interface of the co-flow causes polymers forming at the top and bottom wall in between two streams. The polymers clog the channel and causes jetting. Jetting is not desired for production of MAP gel particles because droplets with unpredictable sizes are produced under jetting condition, resulting in a polydisperse droplet population. Polymerization poses more challenges when we are trying to make MAP gel droplets with 8-arm PEG-VS because it reacts faster.

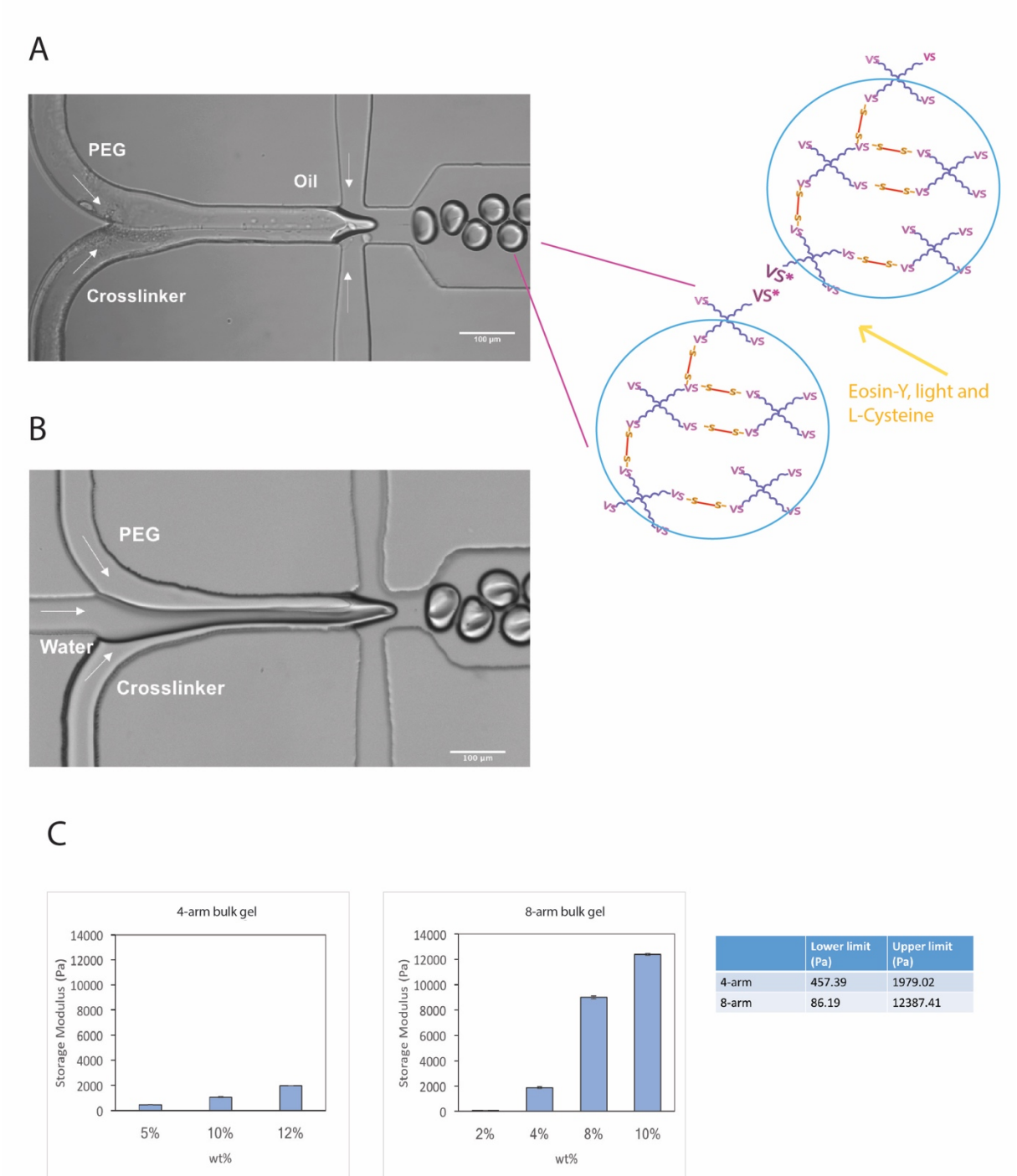

	Lower limit (Pa)	Upper limit (Pa)
4-arm	457.39	1979.02
8-arm	86.19	12387.41

Fig.1: A. Left: droplet generation part of 2-inlet device under microscope (10x objective). Right: Schematic drawing showing crosslinking of 4-arm PEG and di-thiol crosslinker in a single droplet and

annealing by light based radical polymerization. (Purple VS* indicates activated vinyl sulfone radical). B. droplet generation part of 3-inlet device under microscope (10x objective). C. Storage modulus of 4-arm and 8-arm bulk gel, presented here as mean modulus ± s.d. Upper and lower limit for 4-arm and 8-arm bulk gel are shown in chart. (1C created with Jaekyung Koh).

In order to solve the problem of polymerization, we have created a 3-inlet device in which a buffer stream is introduced in between two reactant streams to prevent them from synthesizing polymers in the channel. (Fig.1B) The middle stream can separate the region of transverse diffusion for the two reactant streams and slow down polymerization in the channel. Middle stream with a certain width prevents polymerization from happening for over 8 hours. The width of the middle stream can be tuned by adjusting its viscosity and flow rates. Moreover, 3-inlet device can produce droplets with similar properties of the 2-inlet device at the same aqueous to oil flow rates. With its ability to slow down polymerization and replicate droplet production in 2-inlet device, 3-inlet device is ideal for continuous mass production of MAP gel microparticles for a long time.

MAP gel enables a novel bottom-up approach to form gel scaffolds that provides stable mechanical support to different sites and promote cell migration and tissue integration, which is important for tissue engineering. Wider stiffness range empowers the favorable features of MAP gel to be applied to more research and clinical studies, including cardiac tissue regeneration, brain repair [13] . Mass production of MAP gel is needed to increase reproducibility of both *in vitro* and *in vivo* study. Therefore, our autonomous device can reduce the researchers' effort in preparing the material. The system can also be applied to other systems where polymerization is a problem.

II. Consistent droplet generation profile in 3-inlet device and 2-inlet device

We have tested 3-inlet device on producing MAP gel droplets of different mass concentrations and PEG-VS molecules. Different configurations of the multi-phase flow (Fig.2E) were shown at different flow rates of pre-gel solutions and pinching oil. In the non-jetting region, monodisperse droplets were

generated either through dripping or squeezing regime. (Fig.2B) Different sizes of droplets was generated by tuning the ratio of the flow rates of pre-gel solutions and pinching oil. In the jetting region, aqueous phase is dragged to the downstream by oil phase and broken into droplets due to surface tension. Droplets are of different size compared to non-jetting regime. (Fig.2C) In the polydispersity region, pressure from oil pinching is larger than pressure created by aqueous flow at the intersection. High pressure causes instability in droplet formation, resulting in different sizes of droplets(Fig.2D) We were able to achieve stable droplet formation at the same conditions as 2-inlet device. Comparing 3-inlet device on making 4-arm and 8-arm MAP gel of different mass concentrations, we discovered that configurations at certain flow rates of aqueous and oil phase only depend on the final mass concentration of PEG-VS after all the streams encapsulated into droplets. On the other hand, at a given ratio of flow rates of aqueous phase and oil phase, droplets of similar size were produced. (Fig.2F) We were able to produce 4wt% 8-arm MAP gel droplets with a size ranged from 58 ~ 107μm, corresponding to estimated pore diameters of 15 ~ 20μm in MAP gel network after annealing.[4]

III. Middle stream slow down polymerization in 3-inlet device for longer production time

In the 2-inlet device, polymerization usually happens at the top and bottom walls because of transverse diffusion. The flow profile at the interface (y=0) is approximately parabolic in x, with maximum velocity in the middle of the channel (x=0), and zero velocity at the walls (x = +/- H/2). With lower Péclet number, the flow near the walls has larger spatial extent of transverse diffusive mixing than that in the center. (Fig.3A) The curvature of the transverse diffusion region is due to different scaling of transverse diffusion near the wall and in the center. The width of the reaction-diffusion zone scales as the 1/3 power of both z and average velocity near the top and bottom walls, while the region scales as the 1/2 power of z and average velocity at the center of the channel. [14] Accumulation of polymers at the

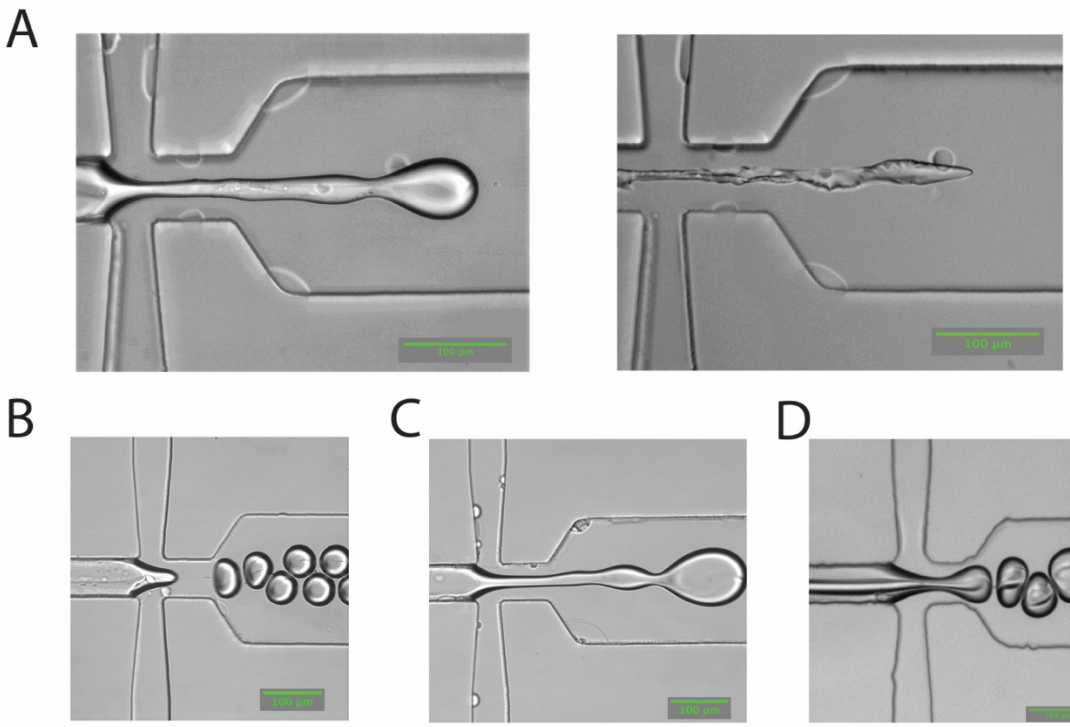
A
B
C
D
100 µm

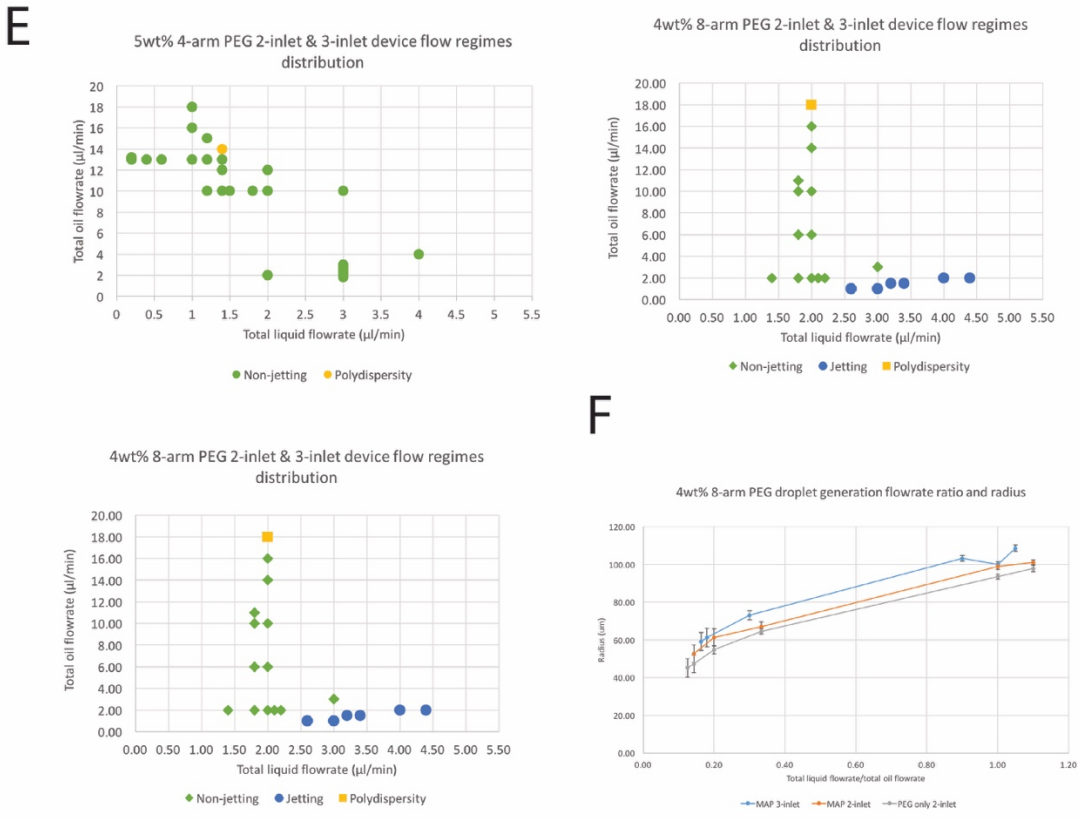
E
5wt% 4-arm PEG 2-inlet & 3-inlet device flow regimes distribution
Total oil flowrate (µl/min)
Total liquid flowrate (µl/min)
Non-jetting
Polydispersity
4wt% 8-arm PEG 2-inlet & 3-inlet device flow regimes distribution
Total oil flowrate (µl/min)
Total liquid flowrate (µl/min)
Non-jetting
Jetting
Polydispersity
4wt% 8-arm PEG 2-inlet & 3-inlet device flow regimes distribution
Total oil flowrate (µl/min)
Total liquid flowrate (µl/min)
Non-jetting
Jetting
Polydispersity
F
4wt% 8-arm PEG droplet generation flowrate ratio and radius
Radius (µm)
Total liquid flowrate/total oil flowrate
MAP 3-inlet
MAP 2-inlet
PEG only 2-inlet

Fig 2: A, polymers accumulated in the channel and caused jetting. Images are taken under microscope (20x). B, droplet generation regime under microscope (10x objective). C, jetting regime caused by flow rate under microscope (10x objective). D, polydispersity regime under microscope (10x objective). E, Distribution of flow regimes at different combination of flow rates. Droplet generation (non-jetting) is smaller for 8-arm and higher wt% MAP gel than 4-arm and lower wt% MAP gel. F, Droplets produced from 3-inlet are of similar size as those produced from 2-inlet and operation without cross-linker. Size is represented as mean radius ± s.d.

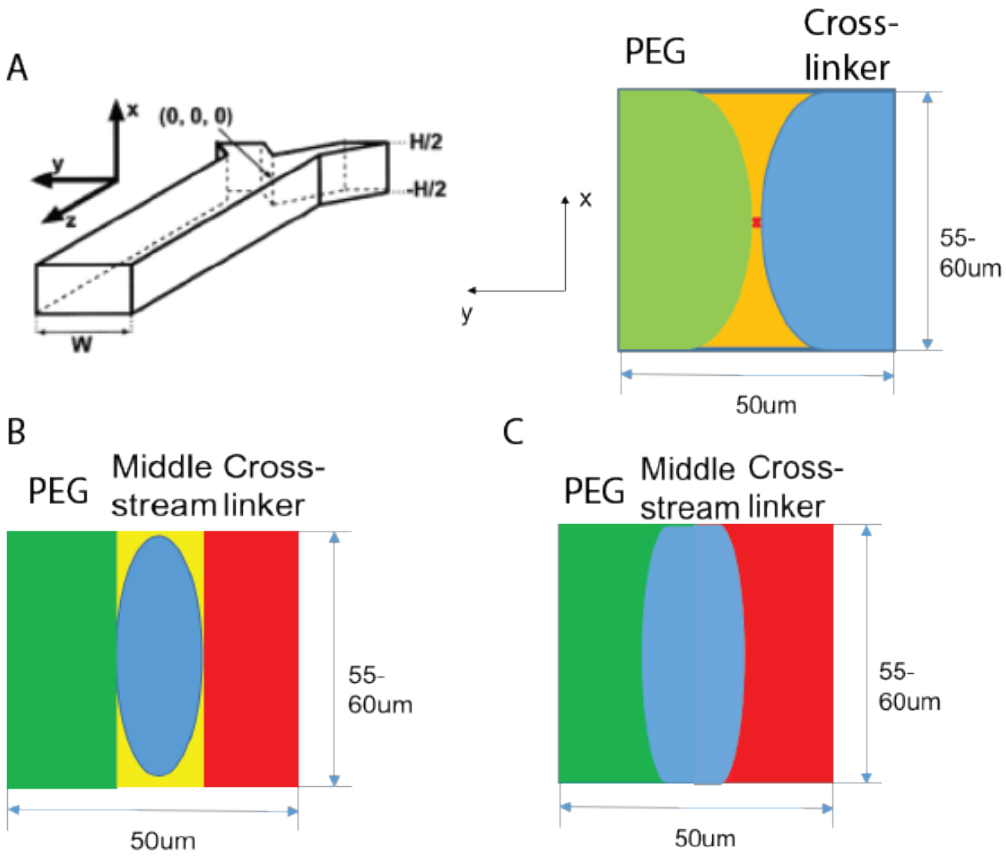

Fig.3: A. Left: 3D graph indicating channel dimensions in 2-inlet device. x axis is along the height of channel, y axis goes along the width, z axis points to the direction of flow.[14] Right: 2D graph showing fluid profile at the x-y cross-section of 2-inlet device. Yellow area indicates transverse diffusion region. B. 2D graph showing fluid profile at the x-y cross-section of 3-inlet device when middle stream is not wide enough to separate the two side streams. Yellow area indicates transverse diffusion region. C.

2D graph showing fluid profile at the x-y cross-section of 3-inlet device when middle stream is wide enough to separate the two side streams.

wall blocked the channel and caused jetting of the aqueous flow. In the 3-inlet device, there are two different situations depending on the width of the middle stream. When the middle stream is not wide enough to prevent the diffusion regions from overlapping, the middle stream is encapsulated by the two side streams and polymers still form on top and bottom walls but the polymerization process is slowed down. (Fig.3B) When the middle stream is wide enough to separate the two streams, the diffusion regions do not overlap and no polymerization happens in the channel. (Fig.3C)

Using the 3-inlet device with water as the middle stream, we were able to achieve stable production of 5wt% 4-arm MAP gel droplets for 8.5 hours without any polymers formed in the channel, which was more than 4 times longer than using previous 2-inlet device. (Fig.4A) With the same flow rates of pre-gel solutions and pinching oil, the size of the droplets generated from our device stayed monodisperse (cv<5%) throughout the generation. (Fig.4B, C) Therefore, the final population of droplets was monodisperse in one production.

Polymerization was slowed down in the production of 5wt% 8-arm MAP gel droplets. Our 3-inlet device ran more than 3 times longer (210 mins) before polymers in the channel caused aqueous stream to jet than previous 2-inlet device(60mins) on generating similar mass concentration of MAP gel (4wt% 8-arm). Considering similar widths (Fig.5A) of the middle channel in the production of 4-arm MAP gel and 8-arm MAP gel, we assume that the diffusion extent of 8-arm PEG-VS is larger than that of 4-arm PEG-VS. Therefore, wider middle stream is required to decrease polymerization in production of 8-arm MAP gel.

A

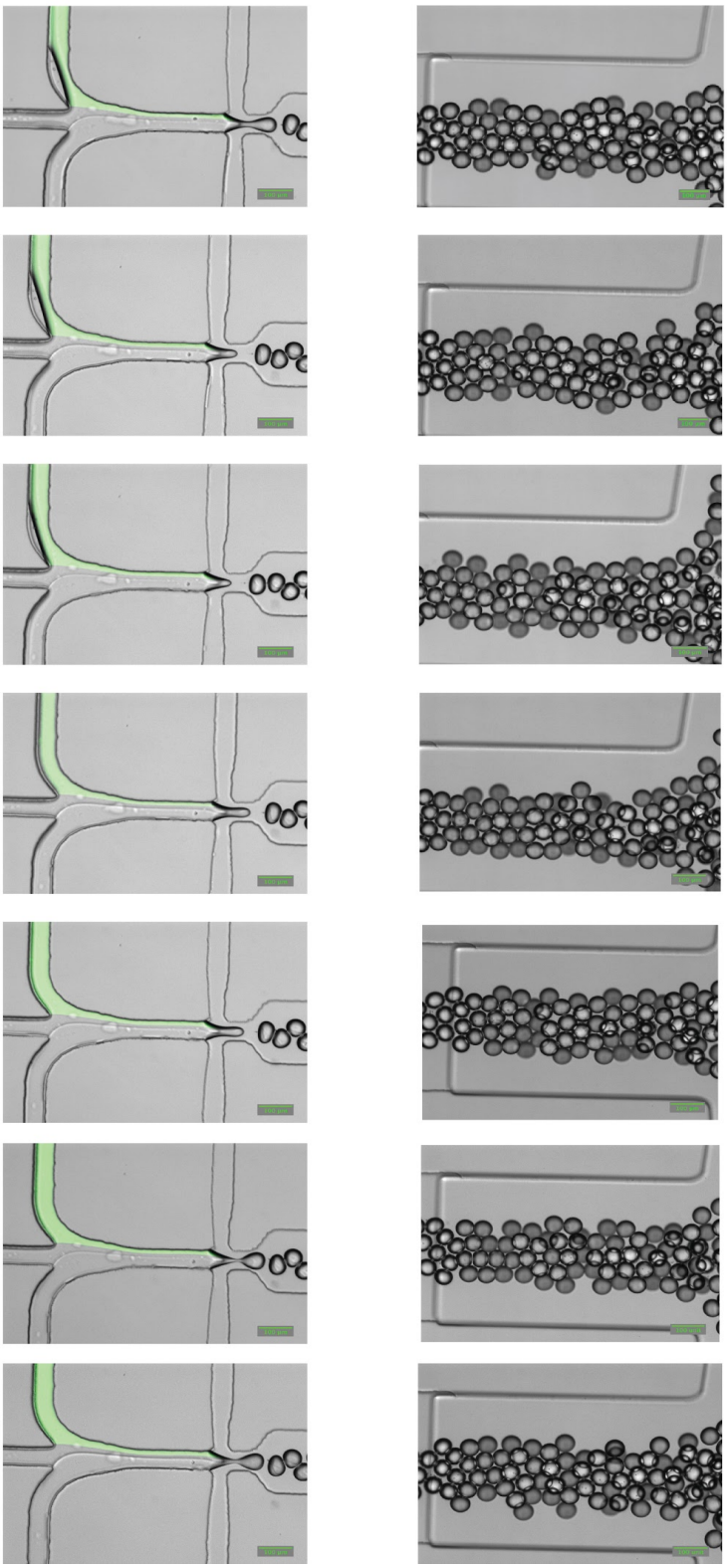

After 1 hour

After 2 hours

After 3 hours

After 4.3 hours

After 6.5 hours

After 7.3 hours

After 8 hours

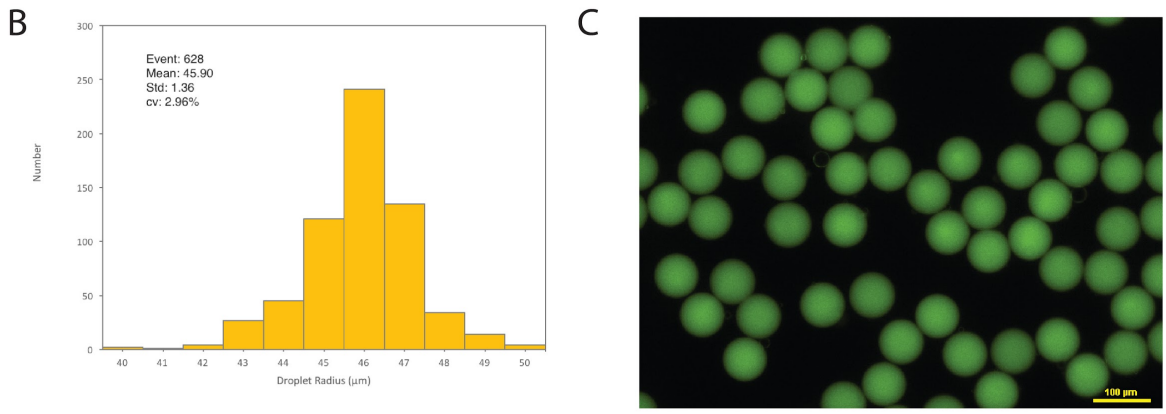

Fig. 4: A, 3-inlet device produce 5wt% 4-arm MAP gel droplets for 8.5 hours without causing polymerization. Images of droplet generation and collection every 1-2 hours. Upper stream: MMP crosslinker, middle stream: water, lower stream: 4-arm PEG-VS. Aqueous flow rate: 0.7µl/min, oil flow rate: 5µl/min. B, Distribution of droplet size over 8 hours. Number of droplets: 628, mean radius: 45.80µm, standard deviation: 1.36µm, coefficient of variation: 2.96%. C. representative image of monodisperse droplets after swelling (Qv = 4.5). Scale bar in all the above images are 100µm.

On making degradable MAP gel with higher mass concentration, MMP crosslinker solution is oversaturated if prepared as 3X concentrated solution. We adjusted the flow rate of the middle stream to be half of the side streams to avoid oversaturation of degradable crosslinker because it was prepared as 2.5X concentrated solution. However, PEG-VS solution pushed the middle stream and the crosslinker to the side wall. The width of the middle stream was also too small to prevent diffusion of PEG-VS molecule to the side wall and formed polymers there. The device jetted after 1 hour, the same time as 2-inlet device. Therefore, the middle stream should be wide enough in order to slow down polymerization.

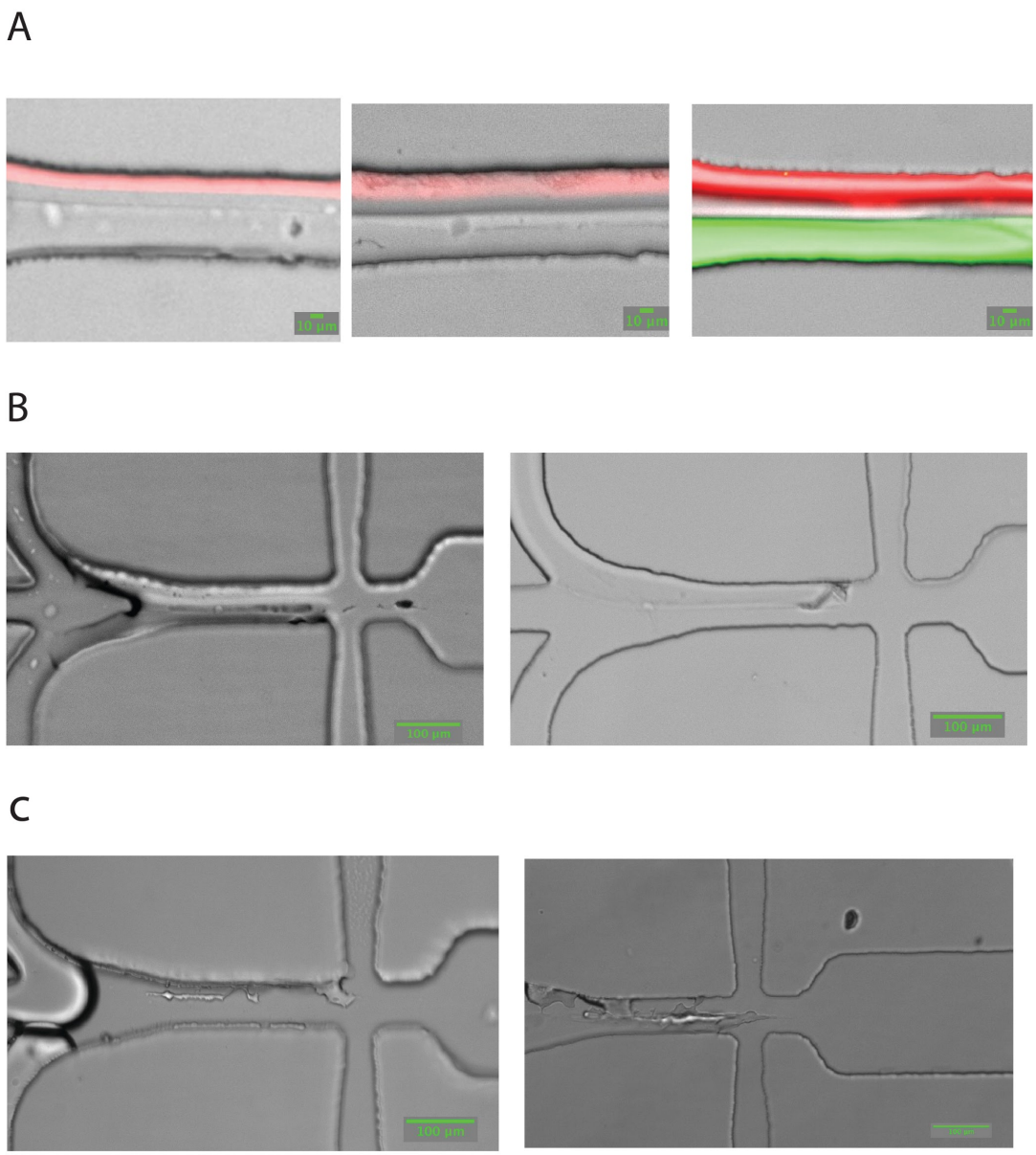

Fig. 5: A, stream width in the co-flow channel for production of: 5wt% 4-arm MAP (left), 5wt% 8-arm MAP (center), 8wt% 8-arm MAP (right). Upper stream: cross-linker, middle stream: buffer solution, lower stream: PEG-VS solution. The width of middle channel is: 10.4μm (left), 8.68μm (center), 14.95μm (right). B, Images of co-flow channel after production of 5wt% 8-arm MAP gel. Middle buffer solution is water (left) and 67% (v/v) linear PEG solution. C, Images of co-flow channel after production of 5wt% 8-arm MAP gel. Middle buffer solution is water (left) and 67% (v/v) linear PEG solution.

IV. Wider middle stream increases production time of stiffer MAP gel further

When fluids flow steadily side by side, at low Reynold's number, in a microchannel, its width is directly proportional to the product of its viscosity and volumetric flow rate.[15, 16] Based on the relationship, we developed a strategy to increase the width of the middle stream by changing its viscosity with different volume concentration of linear PEG molecules (Sigma, MW = 200). Since linear PEG is inert to both vinyl sulfone group and thiol group, it will not interfere with the crosslinking reaction of MAP gel formation. After complete gelation inside the droplets and the emulsion is broken by a buffer, linear PEG can diffuse out of the gel network due to its small size compared to the multi-arm PEG (MW = 20,000). However, aqueous phase of higher viscosity tends to have a smaller non-jetting region. (Fig.2D) Therefore, we adjusted viscosity of the middle stream in order to minimize polymerization while maximizing the region of droplet formation.

In order to achieve a longer production time for 5wt% 8-arm MAP gel, viscosity of the middle stream was adjusted to approximate to PEG-VS solution by using a 67% (v/v) linear PEG liquid. The middle stream was about 2 times wider than the water middle stream used before. After running for 6 hours, the device did not jet and the area of polymers formed in the channel smaller than before when we use a water middle stream. Most importantly, there were no polymers accumulated at the orifice near the breakup point of droplet formation, which was observed in jetting conditions to interfere segmentation of the aqueous stream. (Fig. 5A, B) Except for polydisperse droplet formation around 3.75% of the observation time, droplet production stays monodisperse. Device automatically recovers back to monodisperse droplet formation after about 30s. Therefore, the final population of droplets was considered monodisperse.

Middle stream with same viscosity was tested on making 8wt% 8-arm MAP gel as well. The middle stream became wider while the width of the PEG-VS stream became smaller. (Fig.5C) With increased width of the middle and cross-linker streams, polymers do not form at the side walls and

shift towards the center of the channel. In this case, the device ran more than 2 times longer than previous setups.

Overall, 3-inlet device is shown to slow down polymerization in the channel and have stable droplet formation for a longer time than 2-inlet device does. (Fig.6) The stream width is critical in minimizing polymerization.

	2-inlet	3-inlet (MMP cross-linker)	3-inlet (PEG cross-linker)
5wt% 4-arm	120 min	>480 min	
4wt% 8-arm	60 min	>150 min	
5wt% 8-arm			>360 min
8wt% 8-arm	60 min	60 min	140 min
10wt% 8-arm	40 min		

Fig.6: The table shows operation time of the device on making MAP gel of different chemical properties before polymers causes jetting in device. “>” indicates situations when solutions ran out before polymers lead to jetting in the device.

V. Droplets produced from 3-inlet device annealed and showed gel-like properties

The annealing force of MAP gel were determined by their storage modulus. Storage modulus of micro gel droplet solution is higher after annealing than before annealing. Moreover, storage modulus increases nearly 3-fold after 10 mins of incubation, showing annealing reaction over time. Comparing annealed 5wt% 4-arm MAP gel and 8wt% 8-arm MAP gel, we found a 4 time increase in storage modulus. Because there are 3.2 times more free vinyl sulfone group for 8wt% 8-arm MAP gel

than 5wt% 4-arm MAP gel, the result is consistent with theoretical calculation. (Fig.7) The result shows the capability of 3-inlet device in producing functional MAP gel droplets. Higher storage modulus could be due to higher stiffness of the microparticles or stronger annealing force.

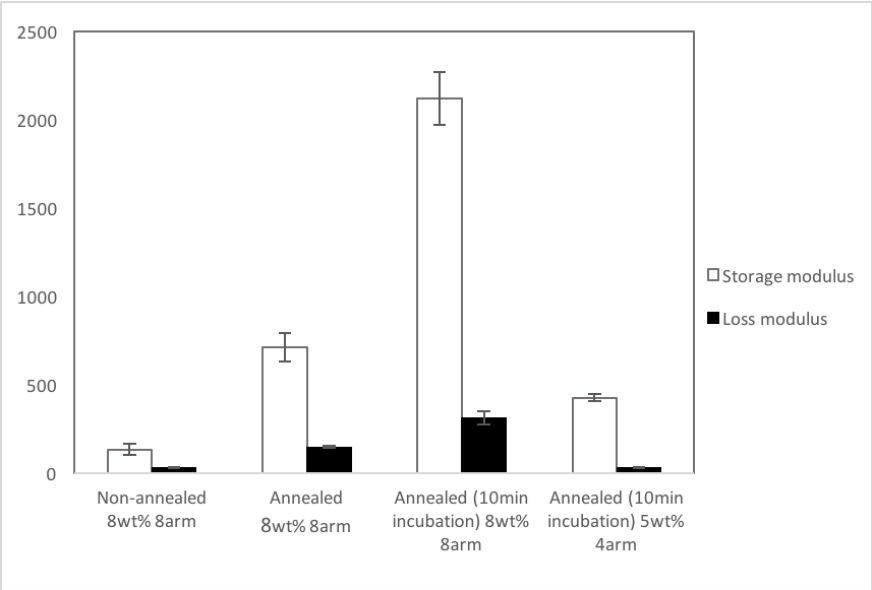

Fig.7: Graph of storage and loss modulus of 8wt% 8-arm MAP gel and 5wt% 4-arm MAP gel. The modulus is represented as mean value (from 0.1-1Hz) ± s.d.

VI. Materials and method

Microfluidic device design and fabrication

Microfluidic flow focusing droplet generators were fabricated using soft lithography as previously described. In short, master molds were fabricated on mechanical grade silicon wafers (University wafer) using KMPR 1025 or 1050 photoresist (Microchem).

Devices were molded on the master molds using poly(dimethyl)siloxane (PDMS) Sylgard 184 kit (Dow Corning) with polymer and curing agent mixed at a 10:1 mass ratio. After degassed, the molding material was incubated for at least 6 hours at 65°C. Inlets and outlets were punched and the

PDMS mold was bonded to a glass microscope slide (VWR) with oxygen plasma at 500 mTorr and 75W for 15 seconds to enclose the channel. After channel sealing, the device was incubated at 65°C to reinforce bonding. Rain-X was injected to cover the channel and react for 1h hour at room temperature. The channels were then dried by air followed by desiccation overnight.

MAP gel building block generation using microfluidics droplet segmentation

MAP gel microparticles were generated using a microfluidic flow focusing device by water-in-oil emulsion. The aqueous phase is a 1:1 volume mixture of two parts: (i) multi-arm PEG-VS (20 kDa) in 300 mM triethanolamine (Sigma), pH 8.25, (ii) di-cysteine modified Matrix Metallo-protease (MMP) (Ac-GCRDGPQGIWGQDRCG-NH2) (Genscript) substrate or PEG-dithiol (1 kDa) pre-reacted with 10 μM Alexa-fluor 568-maleimide (Life Technologies). All solutions were sterile- filtered through a 0.2 μm Polyethersulfone (PES) membrane in a leur-lok syringe filter.

Droplet generation was performed at room temperature with an inverted microscope (Nikon eclipse Ti) for a real-time view of droplet quality. Aqueous solutions did not mix until encapsulated into the droplet by oil (Peclet number >10) at the orifice. The oil phase consisted of heavy mineral (Fisher) oil and 0.3% (v/v) Span-80 (Sigma). Downstream of the orifice, a second oil inlet with a higher volume concentration of Span-80 (3% v/v) was added to the continuous oil phase to prevent coalescing. Gel particles then entered a collecting chamber with multiple bifurcations and ultimately exited through a 1mm outlet connected to collection tubes.

Gel droplets were then purified from mineral oil by being washed with HEPES buffered saline pH 7.4 with 10 mM CaCl2 and 0.01% and pelleting in a table top centrifuge at 3,500 x g for 5 mins. The micro-gel droplets were then allowed to swell in HEPES buffer overnight at room temperature.

Microfluidic flow regime characterization

To determine the flow of droplet segmentation, device performance was monitored in real time using Nikon eclipse Ti and NIS-Elements microscope imaging software. The device is usually initiated

by the following: (a) Oil phase is infused at a flow rate of 5 µl/min until all air has been flushed out of the device, (b) aqueous phase is injected at flow rates that can overcome the pressure of oil phase at the intersection, usually resulting in a continuous flow of the aqueous phase into the oil phase, (c) carefully slow down the aqueous phase and oil phase if necessary to obtain droplet formation.

For characterization of flow regimes (non-jetting, jetting and polydispersity), device was observed for 15 minutes at each combination of flow rates and the flow configuration is recorded if persisted through time. Images of droplets in the collection chamber were captured if there was droplet formation. For long-time operation of device to observe polymerization in the channel, images of droplet formation and collection were captured every hour. Size and polydispersity of droplets were then analyzed by FIJI and MATLAB.

Synthesis of MAP scaffolds from micro-gel droplets

Fully swollen and equilibrated micro-gel droplets were pelleted at 3,500 x g for 5 minutes, while excess buffer (HEPES pH 7.4 + 10 mM CaCl2) was removed by drying with a cleanroom wipe. Subsequently, micro-gel droplets were doped with equal volume of 2X E-L solution (10 µM Eosin Y and 500 µM L-Cysteine in HEPES) at 4°C overnight. Annealing was initiated by exposure to white light for 1 minute and then subjected to at least 10 minutes of incubation for rheology test.

Rheology measurement for stiffness of bulk non-porous gel

To determine the relationship between stiffness and mass concentration for 4-arm and 8-arm MAP gel material, storage modulus of macroscale non-porous gel with the same chemical composition was measured by rheometer (TA instrument). 20µL of PEG-VS bulk solution was mixed with 20µL crosslinker solution, vortexed briefly, and then injected between two glass slides with a spacing of 1mm for incubation at 37°C for 2 hours. The gel pellets were then allowed to swell in PBS buffer at room temperature overnight. Three gel pellets were prepared for each chemical composition. A frequency sweep (0.1-10Hz) was then performed on the fully swollen and equilibrated non-porous gel.

Storage modulus for each chemical composition was calculated by obtaining the mean storage modulus for 0.1-1Hz.

Rheology technique for MAP gel annealing force

Frequency sweep (0.1-10Hz) was performed on the pre-annealed micro-gel particles and post-annealed micro-gel particles to determine the annealing force. For pre-annealed building blocks, 50 µL of MAP building blocks was injected between two 8mm rheological discs at a spacing of 1.8 mm. Frequency sweep was performed right after injection. For post-annealed scaffold measurement, the gel building blocks were first doped with E-L solution overnight. 50 µl of MAP building blocks was injected between two 8mm rheological discs at a spacing of 1.8mm. The gel was exposed to white light for 1 minute and then partially annealed for 10 minutes. Frequency sweep was performed right after injection and 10 minutes of incubation. Storage modulus for each chemical composition was determined by taking the average of the storage modulus from 0.1-1Hz.

VII. Conclusion and future directions

A wider range of stiffness to enables a variety of new applications of MAP gel material. It is shown that 8-arm MAP gel is stiffer and have stronger annealing force than 4-arm MAP gel in both bulk and porous form that it can raise the upper limit of current material. However, production of MAP gel is limited by polymerization in the channel, leading to jetting conditions and unstable droplet formation

Here we introduce a 3-inlet device which adds a middle buffer stream to minimize transverse diffusion mixing of the two reactant streams. Our system is shown to slow down polymerization and increase non-interrupted production time of 5wt% 4-arm MAP gel, 5wt% 8-arm MAP gel and 8wt% 8-arm MAP gel. The width of middle stream can be tuned by changing the viscosity. Wider width has shown promising results in extending the production time of stiffer MAP gel. The system introduces an approach to achieve a larger scale and less labor-intensive fabrication of MAP gel, which will

increase the reproducibility of research studies using MAP gel. Moreover, 8-arm MAP gel expand the stiffness range of the material for broader applications.

However, more investigations should be conducted to identify the critical stream width which can prevent polymerization for higher wt% MAP gel without getting into the jetting regime and oversaturate MMP cross-linker solution. On the other hand, more samples of MAP gel of different mass concentration and PEG-VS material need to be tested for accurate annealing force.

3-inlet device is not the only approach to solve the problem of interrupted production of MAP gel. A step-emulsification combined with pH adjustment has the potential to generate very viscous MAP gel droplets while achieving a much higher throughput (100μl/min). Since no gelation is shown in 4-arm and 8-arm pre-gel mixture at pH=1.2 after 4 hours, the two reactants can be injected as a mixture into the step emulsification device without polymerization, with its pH then raised by downstream oil of basic pH to initiate reaction.

With its microporosity and injectability, MAP gel is an ideal material for tissue regeneration, stem cell delivery and 3-D cell culture. Mass production of the MAP gel with a wide range of stiffness and size will help bringing a variety of clinical and research studies to a new level.

VIII. Reference

1. El-Sherbiny, I. M. & Yacoub, M. H. Hydrogel scaffolds for tissue engineering: Progress and challenges. *Glob Cardiol Sci Pract* **2013,** 316–342 (2013).

2. Alijotas-Reig, J., Fernández-Figueras, M. T. & Puig, L. Late-onset inflammatory adverse reactions related to soft tissue filler injections. *Clin. Rev. Allergy Immunol.* **45,** 97–108 (2013).

3. Sokic, S., Christenson, M., Larson, J. & Papavasiliou, G. In situ generation of cell-laden porous MMP-sensitive PEGDA hydrogels by gelatin leaching. *Macromol. Biosci.* **14,** 731–739 (2014).

4. Griffin, D. R., Weaver, W. M., Scumpia, P. O., Di Carlo, D. & Segura, T. Accelerated wound healing by injectable microporous gel scaffolds assembled from annealed building blocks. *Nat. Mater.* **14,** 737–744 (2015).

5. Sideris, E. *et al.* Particle Hydrogels Based on Hyaluronic Acid Building Blocks. *ACS Biomaterials Science & Engineering* **2,** 2034–2041 (2016).

6. Atzet, S., Curtin, S., Trinh, P., Bryant, S. & Ratner, B. Degradable poly(2-hydroxyethyl methacrylate)-co-polycaprolactone hydrogels for tissue engineering scaffolds. *Biomacromolecules* **9,** 3370–3377 (2008).

7. Madden, L. R. *et al.* Proangiogenic scaffolds as functional templates for cardiac tissue engineering. *Proc. Natl. Acad. Sci. U. S. A.* **107,** 15211–15216 (2010).

8. Matsuzaki, S., Darcha, C., Pouly, J.-L. & Canis, M. Effects of matrix stiffness on epithelial to mesenchymal transition-like processes of endometrial epithelial cells: Implications for the pathogenesis of endometriosis. *Sci. Rep.* **7,** 44616 (2017).

9. Blakney, A. K., Swartzlander, M. D. & Bryant, S. J. The effects of substrate stiffness on the in vitro activation of macrophages and in vivo host response to poly(ethylene glycol)-based hydrogels. *J. Biomed. Mater. Res. A* **100,** 1375–1386 (2012).

10. Chang, F.-C. *et al.* PEG-chitosan hydrogel with tunable stiffness for study of drug response of breast cancer cells. *Polymers* **8,** (2016).

11. Engler, A. J., Sen, S., Sweeney, H. L. & Discher, D. E. Matrix elasticity directs stem cell lineage specification. *Cell* **126,** 677–689 (2006).

12. Huebsch, N. *et al.* Harnessing traction-mediated manipulation of the cell/matrix interface to control stem-cell fate. *Nat. Mater.* **9,** 518–526 (2010).

13. Nih, L. R., Carmichael, S. T. & Segura, T. Hydrogels for brain repair after stroke: an emerging treatment option. *Curr. Opin. Biotechnol.* **40,** 155–163 (2016).

14. Ismagilov, R. F., Stroock, A. D., Kenis, P. J. A., Whitesides, G. & Stone, H. A. Experimental and theoretical scaling laws for transverse diffusive broadening in two-phase laminar flows in microchannels. *Appl. Phys. Lett.* **76,** 2376–2378 (2000).

15. Dambrine, J., Géraud, B. & Salmon, J.-B. Interdiffusion of liquids of different viscosities in a microchannel. *New J. Phys.* **11,** 075015 (2009).

16. Stiles, P. J. & Fletcher, D. F. Hydrodynamic control of the interface between two liquids flowing through a horizontal or vertical microchannel. *Lab Chip* **4,** 121–124 (2004).